Quench Localization in Superconducting Radio-frequency Cavities

Ramesh Adhikari*
Department of Physics, Berea College, Berea, KY 40404

Elvin Harms†
Fermi National Accelerator Laboratory, Batavia, IL 60510
(Dated: August 19, 2010)

Superconducting Radio-frequency (SRF) cavities are the accelerating components for the next generation of particle accelerators. Unlike the normal-conducting cavities, the SRF cavities can stand a high electric field gradient (up to 60 MV/m for niobium) with very low dissipation of the rf power.Cavities that perform at the accelerating gradient of 30-35 MV/m are the current state-of-the-art. Since, the cavities installed in an accelerator must demonstrate no quenches during routine high gradient operation, limitations to such performance must be identified and removed entirely during their manufacturing and testing. Such a test can be performed with a cavity in a helium bath. The second sound generated from the quench on cavity can be used as a signal to identify the quench location. This literature describes a method based on trilateration to predict the location of the quench on a single cell cavity which was verified by the complementary experimental observations from Resistance Thermal Detectors (RTDs)

I. INTRODUCTION

During 20th century various development in particle physics occurred, including the development of Standard Model, discovery of quarks and neutrinos, etc. Still, some of the fundamental issues like the Higgs mechanisms and the existence of supersymmetric particles are still unknown. While the Large Hadron Collider at CERN is colliding proton-proton beams to answer the fundamental questions within the Standard Model, it is general agreement in the high energy physics community that a lepton collider would be a complement to address these fundamental questions. Therefore, various high energy electron-positron accelerators are underway their construction including European XFEL, International Linear Collider, and so on.

Unlike hadron accelerators, high energy lepton accelerators cannot be circular. When the center of mass energy of the electron-positron in a circular accelerator is above 200GeV, the synchrotron radiation loss will be significant enough (due to its dependence of E^4) that the cost of maintenance of beam energy would be drastically high [1]. Instead of this, linear accelerator can be used to accelerate the leptons.

With linear accelerators, we cannot accelerate the particles like in a circular accelerator by feeding more energy at every cycle. Instead, we have to be able to accelerate the particles as fast within a limited distance. Despite their low power dissipation due to small resistance(10 nΩ at 2K), the cost of operating the accelerating system at low temperature makes superconducting cavities as expensive as normal-conducting cavities. But, the low beam impedance, ability to stand high electromagnetic field, and high conversion efficiency [1] makes the superconducting cavities more preferable than the normal-conducting cavities. It turns out that these superconducting cavities will not only be useful for linear lepton accelerators, but also all the next generation accelerators due to their efficiency.

II. SUPERCONDUCTING RADIO-FREQUENCY (SRF) CAVITIES

Superconducting radio-frequency cavities are made out of niobium (Nb). The critical temperature of Niobium is 9.2K and hence, it performs nicely as a superconductor when placed in a cryomodule filled with liquid helium. There are other high critical temperature (T_c) superconductors but they are not used because of either due to difficulties in transforming them to coils and cables (ceramic superconductors) or inferior performance [1] (high T_c sputter coatings on copper) compared to niobium cavities.

The advantage of superconducting cavities is their high quality factor (Q-factor). For niobium, the Q-factor is 2.7 x 10^{10}, while for the normal conducting cavities, it is between 10^4 - 10^5. This is equivalent to the rf loss by 5 to 6 orders of magnitude and hence most of the power is transferred to the beam or reflected into a load. Nevertheless, there is a physical limit set by the superheating field for the superconductors. The rf magnetic field at the inner surface of the superconducting resonator should stay below the superheating field. , which is about 100-240 mT for pure niobium. This implies that the maximum attainable accelerating gradient, in principle, for the niobium cavities would be about 50-60 MV/m. More constraints on the field is added by the impurities in Niobium itself making the feasible accelerating gradient to be 30-35 MV/m.

Due to the high accelerating gradient a cavity has to stand, the surface of the cavity should be virtually smooth. If there is any physical defect in the cavity, the

*Ramesh Adhikari adhikarir@berea.edu
†Elvin Harms harms@fnal.gov

RF energy that is fed into the cavity for the acceleration of the particle would be absorbed around the location of defect. Niobium is a bad thermal conductor, with thermal conductivity of about 125 $Wm^{-1}K^{-1}$ at 4.2K (RRR = 500). Hence, the absorbed energy at the defect will buildup upon itself and heat the surface of the cavity. As the temperature of the cavity surface increases, the cavity will lose its superconducting state which is defined as quench. The cavity will not perform as designed in this situation. Therefore, the quench detection has been a very important and time consuming part of manufacturing the cavities.

III. SUPERFLUIDITY OF ^4He

A cold test can be done to locate quench on a cavity [2]. For the purpose, a cavity is placed in a helium (Helium II) bath at 2K. Traditionally, quench locations have been identified by attaching Resistance Thermal Detectors (RTDs) on the surface of the cavity. The thermometer that is closest to the quench would show the maximum temperature gradient. This would help us to localize the quench, but the process gets tedious and painstaking while carrying out the test even for few cavities. Another method of detecting quench that could give better idea of quench location is by exploiting the properties of the superfluidity of Helium II.

Normal Helium (^4He) can be found in its liquid state at 4.21K. It is called as He I and it behaves as an ordinary liquid with a small viscosity. When the temperature is lowered to 2.17K Helium I undergoes a transition which does not cost it latent heat [3]. Below that temperature, helium exists as a superfluid and is referred to as He II. Many properties of He II at or below this temperature can be understood in terms of the two-fluid model [4]. Proposed by Tisza(1938), the model suggests that He II behaves as inseparable mixture of superfluid and and normal fluid. This allows the liquid to have ordinary viscosity while flow though narrow channels without any friction. It has been observed that He II is capable of two different motions at the same instant. Each of these motions has its own velocity, say ν_n and ν_s for normal fluid and superfluid respectively. Also, each of its kind of liquid has its own effective mass density, ρ_n and ρ_s. This will allow us to calculate the density of He II as:

$$\rho = \rho_n + \rho_s \tag{1}$$

This property of Helium II that enables us to distribute the effective mass density into two different components will be helpful to determine the properties of the Oscillating Superleak Transducer which is the core of this project.

IV. SECOND SOUND

Due to a higher temperature at the location of quench on the cavity, a disturbance on the neighboring helium occurs which creates the second sound waves.

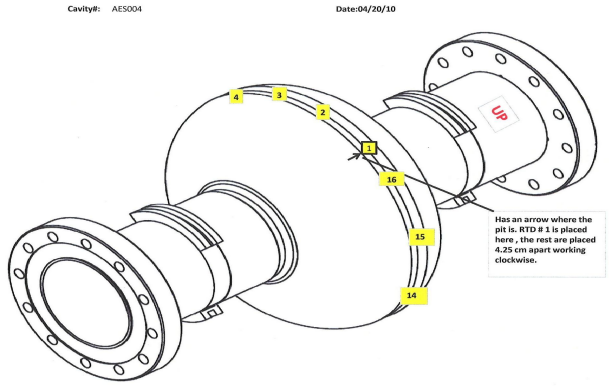

FIG. 1. A drawing of RF cavity. Marked in yellow are locations of resistance temperature detectors (RTDs)

Second sound is a phenomenon where the heat is transferred in a waveform rather than by diffusion. One of the interesting properties of He II is to permit the propagation of thermal waves, analogous to sound waves, which are named as second sound waves[5]. The velocity of second sound in He II is a function of temperature. The velocity vanishes when the temperature heads towards the λ point. λ point is the temperature under which Helium exists as superfluid. The velocity increases sharply from the λ point till it reaches about 2K. The velocity tends to be constant till the temperature lowers down to 1K after which its steeps up again as the temperature heads towards absolute zero. A graphical representation of the second sound velocity behavior is shown in the figure (3).

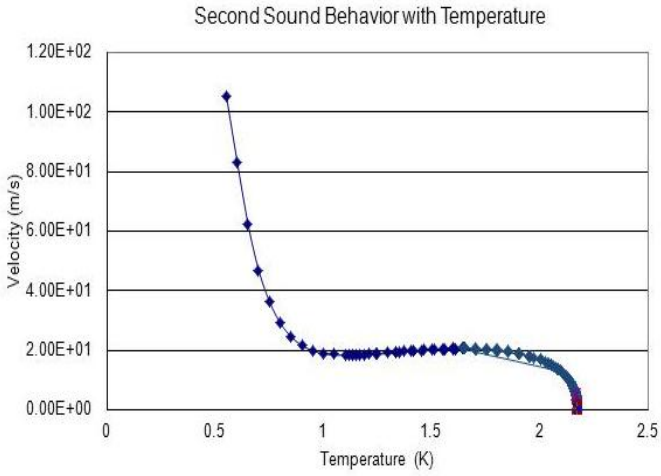

FIG. 2. Temperature response of second sound on its velocity.

V. OSCILLATING SUPERLEAK SECOND SOUND TRANSDUCERS (OSTS)

Oscillating Superconducting Transducers(OSTs) are cylindrical in structure. One end of the cylinder is closed by a diaphragm which, in our case, is a polycarbonate filter with 0.2μm pores. On the other end of the cylinder, against the diaphragm, a bronze layer of thickness 0.02mm is coated on the aluminum wall and is connected to a SMA connector. At this end, second sound signal is converted into electrical signal and transmitted to an oscilloscope taking advantage of the capacitor-like interaction between the diaphragm and the bronze coated wall.

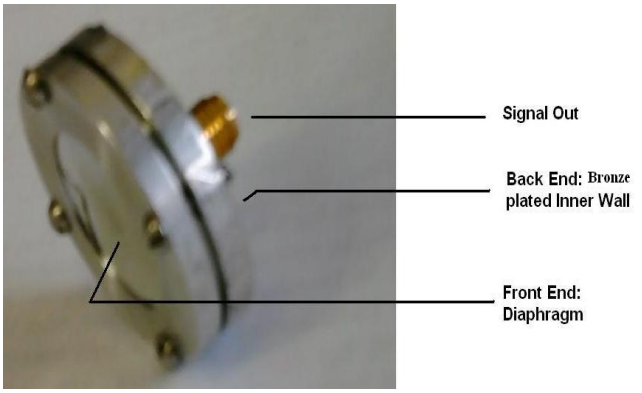

FIG. 3. Oscillating Superleak Transducer

For theoretical calculation and quantifying its performance, a transducer can be modeled as a Helmholtz Resonator [6]. Due to the second sound wave coming in through He II, flexural waves are created on the diaphragm. If the average distance (d) between the diaphragm and the back plate is very small (d$\ll\lambda$) compared to the wavelength (λ) of the flexural wave on diaphragm, then all the parts of the diaphragm will oscillate in phase. For this situation, the diaphragm can be considered as a rigid piston enclosing a volume (v = S.d) of excitation gas, where "S" is the cross-sectional area of the diaphragm. This system, at sufficiently low frequency will satisfy the condition ($\lambda \gg d$) and hence, can be treated as a Helmholtz resonator.

A Helmholtz resonator can be represented by a simple series resonance circuit [6]. This model allows us to write the behavior of the system that includes interaction of second sound and diaphragm in terms of total acoustic compliance C_s as:

$$\frac{1}{C_s} = \frac{1}{C_l} + \frac{1}{C_d} \tag{2}$$

where, C_l and C_d are the He II and diaphragm compliances, respectively. Here, we can see that the total capacitance of the system is equivalent to the total capacitance of the circuit with capacitors in series. Now, we can also find the relationship between diaphragm displacement and the alternating voltage produced by the transducer [6]. This alternate voltage can be transmitted as electric signal.

It should be noted that the use of this transducer is motivated due to its high efficiency performance. As mentioned earlier, He II is defined with two fluid model. The energy densities in first and second sound waves in such a medium can be written as:

$$E_1 = \frac{1}{2}\rho_n \nu_{n1}^2 = \frac{1}{2}\rho_s \nu_{s1}^2 \tag{3}$$

$$E_2 = \frac{1}{2}\rho_n \nu_{n2}^2 + \frac{1}{2}\rho_s \nu_{s2}^2 \tag{4}$$

where, ρ_n and ρ_s and ν_n and ν_s are the mass densities related to normal and superfluid helium, while, 1 and 2 are related to first and second sound, respectively.

From the principle of conservation of momentum:

$$\rho_n \nu_{n2} = -\rho_s \nu_{s2} \tag{5}$$

We can use relations (1) and (4) and divide equation (3) by (2) to derive the efficiency relation for a transducer [6]:

$$\frac{E_2}{E_1} = \frac{\rho_n}{\rho_s}.\left(\frac{\nu_{n2}}{\nu_{n1}}\right)^2 \tag{6}$$

We can now, get rid of the velocity terms from the relation by considering the boundary conditions at the diaphragm:

$$\nu_n = \nu_{n1} + \nu_{n2} = v \tag{7}$$

where, ν is the diaphragm velocity and,

$$\nu_s = \nu_{s1} + \nu_{s2} = 0 \tag{8}$$

From relation (6) and using relations (1), (2) and (4) we can derive:

$$\rho\nu_{n1} = \nu\rho_n \Rightarrow \nu_{n1} = \frac{\nu\rho_n}{\rho} \tag{9}$$

Similarly,

$$\rho\nu_{n2} = \nu\rho_s \Rightarrow \nu_{n2} = \frac{\nu\rho_s}{\rho} \tag{10}$$

Now, using relations (8) and (9) we can reduce equation (5) to:

$$\frac{E2}{E1} = \frac{\rho_s}{\rho_n} \tag{11}$$

For He II, the density of normal fluid is given as [7]:

$$\rho_n = \rho.\left(\frac{T}{T_\lambda}\right)^{5.6} \tag{12}$$

where, T is the temperature and T_λ is the λ point of the superfluid.

As we can see, as we lower the temperature, the normal fluid density decreases and hence from the relation

(1) it can be said that superfluid density increases with decreasing temperature. For such case, we can see that the energy density for second sound in OST is larger then for the first sound and hence more efficient than other kind of transducers like Peshkov transducer [6].

Occurrence of quench can be observed as sudden drop in RF energy coming out of the cavity.When the second sound reaches the transducer, we can also observe an abrupt decrement in the voltage signal as shown in figures (9) and (10). If there are three or more OSTs around the cavity, then various time delays are detected. One can measure the time delays between RF drop and signal detected by OSTs. We know the velocity of the second sound at different temperatures from figure (2). Thus, we can learn about the distance of the quench from each detector. Using a method called trilateration, we can compute the location of the quench.

VI. APPROACH

In first subsection, we can use the general equations for spheres and reduce them to a linear system of equations. This system can be further reduced by using Gaussian elimination and the location of quench can be solved. Another subsection will provide algorithm and simulations from the program based on LabVIEW over the internship period.

VI.1. Trilateration

Let's imagine that the OSTs are located at the center of the spheres of radii which are equivalent to distances between the quench locations and themselves. Now, we can think of all these spheres intersecting with each other at the quench location. For practical reasons, the center of the cavity can be considered to be the origin of the 3D coordinate system that would define the position of all the OST's and also the quench.

For this method, we will need four OSTs to exactly locate the quench. Suppose the location of the OSTs are (x_i, y_i, z_i), where i=1,2,3,4 for four OSTs and quench be located at (x, y, z). Then, the distance between OST and quench would be:

$$(x_i - x)^2 + (y_i - y)^2 + (z_i - z)^2 = r_i^2 \tag{13}$$

Hence, the distance of each OST from the quench will be:
for i=1,

$$(x_1 - x)^2 + (y_1 - y)^2 + (z_1 - z)^2 = r_1^2 \tag{14}$$

for i=2,

$$(x_2 - x)^2 + (y_2 - y)^2 + (z_2 - z)^2 = r_2^2 \tag{15}$$

for i=3,

$$(x_3 - x)^2 + (y_3 - y)^2 + (z_3 - z)^2 = r_3^2 \tag{16}$$

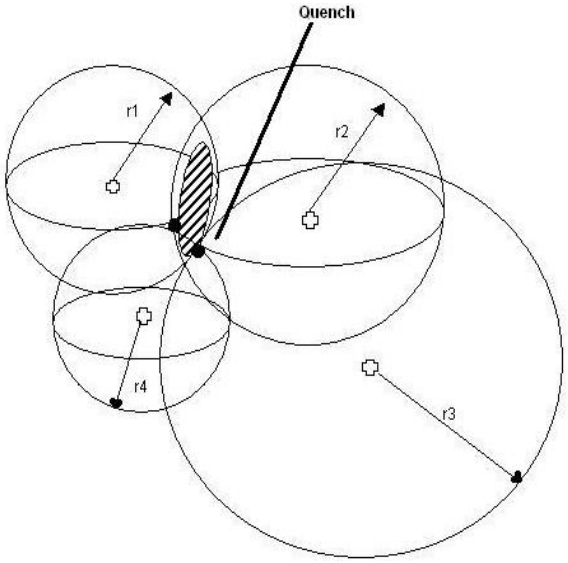

FIG. 4. Trilateration: Visualization of location of quench based on signals from four transducers.

for i=4,

$$(x_4 - x)^2 + (y_4 - y)^2 + (z_4 - z)^2 = r_4^2 \tag{17}$$

We can subtract (14) from (15), (16) and (17) and get rid of the non-linear terms. Then we arrange the left over terms in a matrix form as:

$$M = \begin{bmatrix} 2(x_2 - x_1) & 2(y_2 - y_1) & 2(z_2 - z_1) & s \\ 2(x_3 - x_1) & 2(y_3 - y_1) & 2(z_3 - z_1) & t \\ 2(x_4 - x_1) & 2(y_4 - y_1) & 2(z_4 - z_1) & u \end{bmatrix}$$

where,

$$s = x_2^2 - x_1^2 + y_2^2 - y_1^2 + z_2^2 - z_1^2 - r_2^2 + r_1^2 \tag{18}$$

$$t = x_3^2 - x_1^2 + y_3^2 - y_1^2 + z_3^2 - z_1^2 - r_3^2 + r_1^2 \tag{19}$$

$$u = x_4^2 - x_1^2 + y_4^2 - y_1^2 + z_4^2 - z_1^2 - r_4^2 + r_1^2 \tag{20}$$

We know that the solution of linear equations in this form of matrix can be obtained from reduced row echelon form of the augmented matrix above. This reduced row echelon form of the matrix can be found by Gaussian elimination. For the acknowledgment of the row echelon form of a matrix, suppose the above matrix can be written as:

$$E = \begin{bmatrix} 1 & 0 & 0 & a \\ 0 & 1 & 0 & b \\ 0 & 0 & 1 & c \end{bmatrix}$$

Here, a, b and c can be easily calculated provided that we have the information about

$(x_1, y_1, z_1), (x_2, y_2, z_2), (x_3, y_3, z_3), (x_4, y_4, z_4)$ which are basically the positions of the transducers with respect to the center of the cavity. $r_1, r_2$and r_3 are the distance of the quench from each transducer. The position of the quench (x,y,z) can be calculated as:

$$x = a \tag{21}$$

$$y = b \tag{22}$$

$$z = c \tag{23}$$

Based on this mathematical principle, we developed a program based on LabVIEW that would intake the parameters including co-ordinates of the transducers , velocity of second sound wave and time delay of the second sound signal on each of the four transducers. As a result, the program would output the quench location in 3D space.

VI.2. Software Development

Even though the mathematical principle behind the solution is quite trivial, we will always be in advantage if we can have an automated program that calculates the quench location within a moment. The program can be divided into three distinct sections.

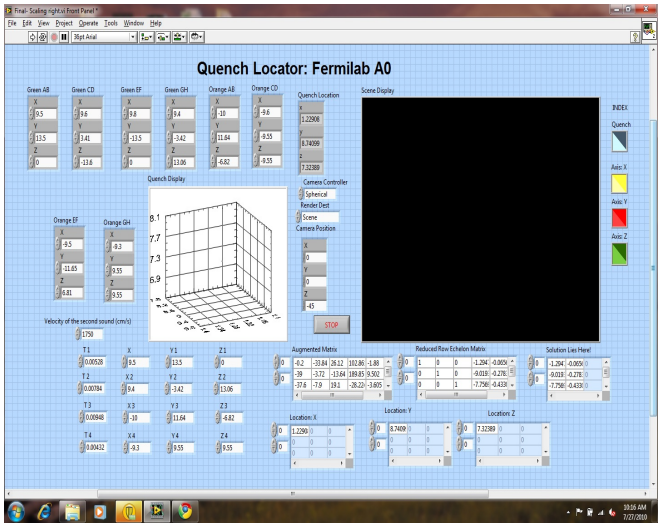

FIG. 5. Screen shot of the developed user interface for entering data.

VI.2.1. Data Intake

The user will need to enter the velocity of the second sound depending on the temperature of the cold test experiment. The time delays can be observed from the oscilloscope that reads the second sound response at different transducers around a cavity, and entered in the program. Also, the program requires the position of four transducers to be entered. These all entries would be rearranged in the program and rearranged as the elements of matrix M.

VI.2.2. Computation

After the inputs are arranged in the form of elements of matrix M, triangulation is performed. For the purpose, a well known Gaussian Elimination method is used. For programming the process, elementary row operations to the augmented matrix is performed and an upper triangular matrix is achieved i.e.

$$\mathbf{M} = \begin{bmatrix} a_{11} & a_{12} & a_{13} & \cdots & a_{1k} & |b_1 \\ a_{21} & a_{22} & a_{23} & \cdots & a_{2k} & |b_2 \\ \cdots & \cdots & \cdots & \ddots & \cdots & |\cdots \\ a_{k1} & a_{k2} & a_{k3} & \cdots & a_{kk} & |b_3 \end{bmatrix} \tag{24}$$

is converted to:

$$\mathbf{e} = \begin{bmatrix} 1 & a_{23} & a_{13} & \cdots & a_{1k} & |b_1^{'} \\ 0 & 1 & a_{23} & \cdots & a_{2k} & |b_2^{'} \\ \cdots & \cdots & \cdots & \ddots & \cdots & |\cdots \\ 0 & 0 & 0 & \cdots & a_{kk} & |b_3^{'} \end{bmatrix} \tag{25}$$

Now, we know the value of the variable (x_k) which is $b_3^{'} - a_{kk}$. For getting values of other variables (x_{k-1}, and so on), we can use following relation [8]:

$$x_i = \frac{1}{a_{i.i}^{'}} \left(b_i^{'} - \sum_{j=i+1}^{k} a_{i.j}^{'} x_j \right) \tag{26}$$

VI.2.3. Display

Due to the complexities in LabVIEW for graphical interface the programming becomes somewhat tedious. 3D picture control of the program provides different option for 3D display but they are not flexible. The designed display may not serve as a complete graphical interface, while the geometries themselves appeared as expected and have good visualization. The display provides a three dimensional display of the quench location in the cavity. The simulated cavity image and the quench location will be displayed on the figure (11) in Experiment section.

VII. EXPERIMENT

The experiment is performed at the temperature at or below 2K. A cold test is set up as shown in figure (6). A

cavity is aligned vertically with some supporting system. The center is cavity is arranged to be at the midpoint between two circular plastic discs. On each of these discs, four OSTs are attached in such a way that the four of these OSTs are on the bottom region of the cavity and four on the top. Each of the OST is marked AB, CD, EF and GH. The OSTs on the bottom region are called orange and on the top regions are called greens.

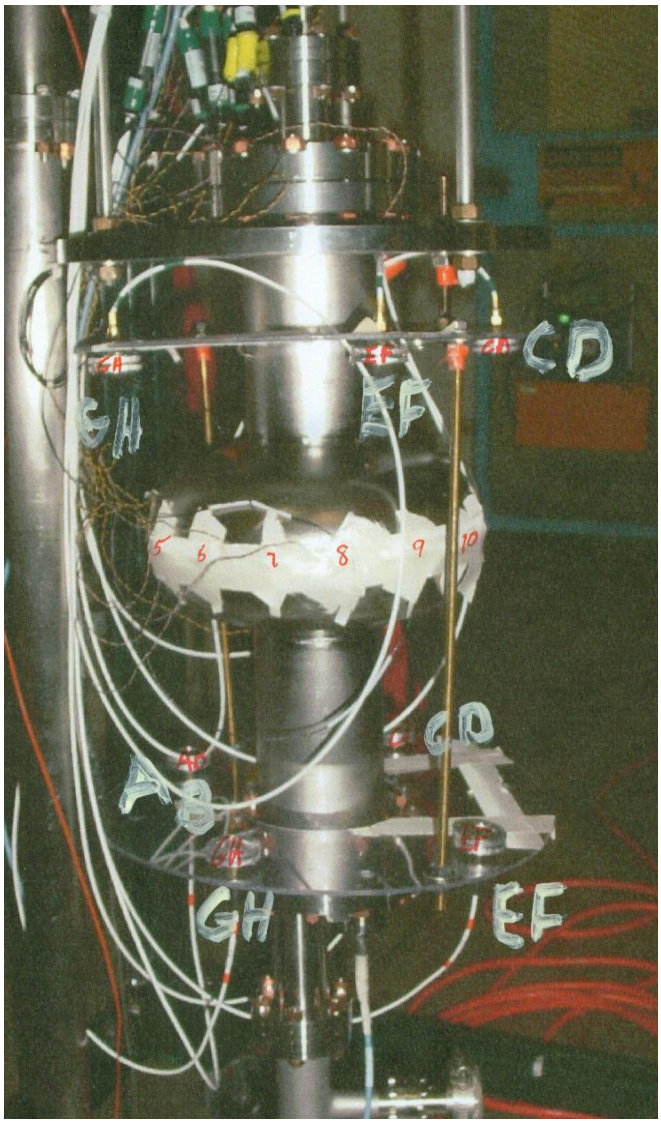

FIG. 6. A cold test setup. A niobium cavity is surrounded by numbered RTDs around its equatorial region. Alphabetical numberings(e.g. GH, EF) are for OSTs.

All the green OSTs are arranged in such a way that they are at the vertices of a rectangle of length 21.5 cm and width of 16.5cm. All the oranges are also aligned on the same fashion, but rotated by 45^0 with respect to the green OSTs. A vertical view of the arrangement of the OSTs would look like figure (7).

The best way to keep the things simple, here, is to define the center of the cavity as the origin of the coordinates that would be used to define the location of the

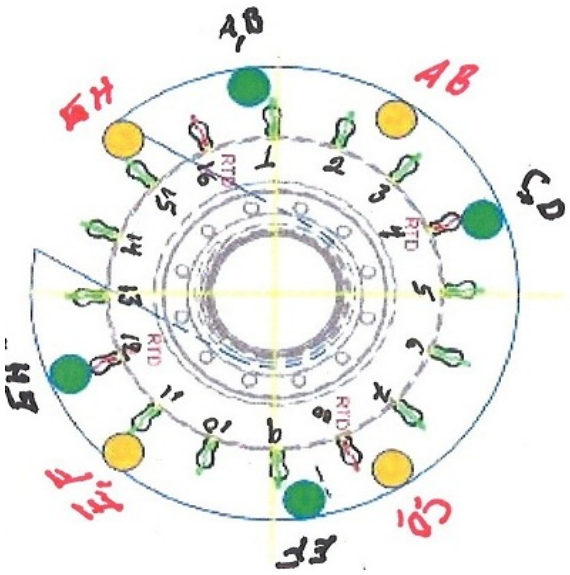

FIG. 7. Vertical view of the alignment of the OSTs during the cold test.

transducers and the quench. To begin with, lets just look at the arrangement of the green transducers. The geometrical arrangement would look like in figure (8). For easier approach, we can define that a green transducer (AB) lies along the horizontal axis.

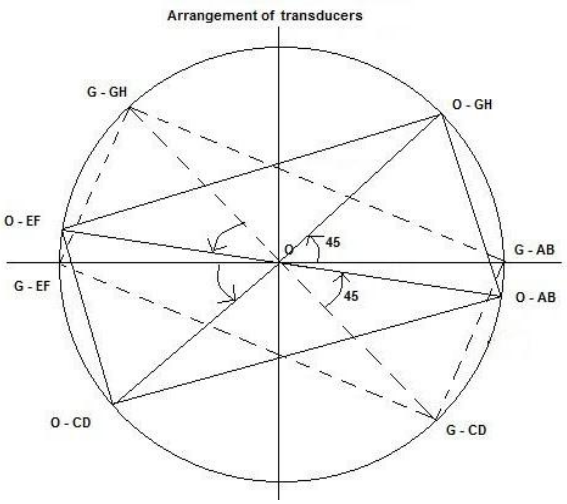

FIG. 8. Geometrical arrangement of the transducers on the vertical test.

We know the separation between each adjacent transducer (length, width and diagonal of the rectangle that contains the transducers). Now, if we just consider the triangle CD, AB and O, we can calculate the angle(γ) between the green transducers AB and CD, based on 'Law of Cosine', as:

$$cos(\gamma) = 1 - \frac{c^2}{2a^2} \tag{27}$$

where, c is the distance between transducers AB and CD,

and a is the half of the distance between AB and EF or CD and GH. In our specific case, the x-axis represents the height of the transducer, while y and z will describe the horizontal plane. For rotation, we will be considering only y and z elements as the x values are always be fixed. Calculations show that $\gamma = 72.4^0$. Now, we can use the rotation matrix (for clockwise rotation) to find the co-ordinates of CD as :

$$\mathbf{CD} = \begin{pmatrix} y' \\ z' \end{pmatrix} = \begin{pmatrix} cos\gamma & sin\gamma \\ -sin\gamma & cos\gamma \end{pmatrix} \begin{pmatrix} y \\ z \end{pmatrix} \tag{28}$$

Here, the yz plane coordinates for AB is (13.5, 0). After rotation on the counter clockwise by 72.4^0, we can get the coordinates for CD as (3.41, -13.6) . We know that the height of AB and CD is 9.5cm and 9.6cm above the origin. Hence, in 3D co-ordinate system, their position would be (9.5, 13.5, 0) and (9.6, 3.41 , -13.6), respectively. We know that EF is diagonally opposite of AB. We can follow the same technique and get its co-ordinate as (9.8, -13.5, 0) and then from rotation - the co-ordinate of GH as (9.4 , -3.42 , 13.06).

The orange transducers GH, AB, CD and EF are rotated counter clockwise by an angle of 45^0 from green AB, CD, EF and GH respectively. For this case, the rotation matrix that can be used will be:

$$\begin{pmatrix} y' \\ z' \end{pmatrix} = \begin{pmatrix} cos\gamma & -sin\gamma \\ sin\gamma & cos\gamma \end{pmatrix} \begin{pmatrix} y \\ z \end{pmatrix} \tag{29}$$

Now, we can figure out the co-ordinates of all the orange transducers. They were found to be (-9.3, 9.55, 9.55), (-10,11.64, -6.82), (-9.6, -9.55, -9.55) and (-9.5, -11.65, 6.81) for GH, AB, CD and EF respectively. These co-ordinates will be useful for the location of the quench, as described by the algorithm in previous section. It needs to be noted that for this system a unit is a centimeter.

Such an arrangement of the OSTs is to maximize the exposed area for the OST's. This will allow us to lower the probability that we will miss any quench location on the cavity. After the second sound reading is performed, a complementary reading is taken from 16 Resistive Thermal Detectors (RTDs) that are attached around the equator of the cavity. This will allow us to double check our findings from OSTs.

VII.1. Observation

The Quench activity is monitored on a oscilloscope which reads data from RF energy and three transducers. The blue line represents the RF field. We can see the quench occurred at the point where the blue graph has a sudden drop. We can also see the readings from the transducers in cyan, green and magenta. Initially, the voltage signal is leveled. As the second sound reaches the diaphragm, it starts to vibrate with the normal fluid while the second sound passes freely. Hence, the capacitance of the transducer fluctuates during the event which we can see on the oscilloscope as a quench. As we are interested on the first disturbance, which is due to first arrival of the second sound, we can measure the time delay between actual quench occurrence and arrival of the second sound at the transducers.

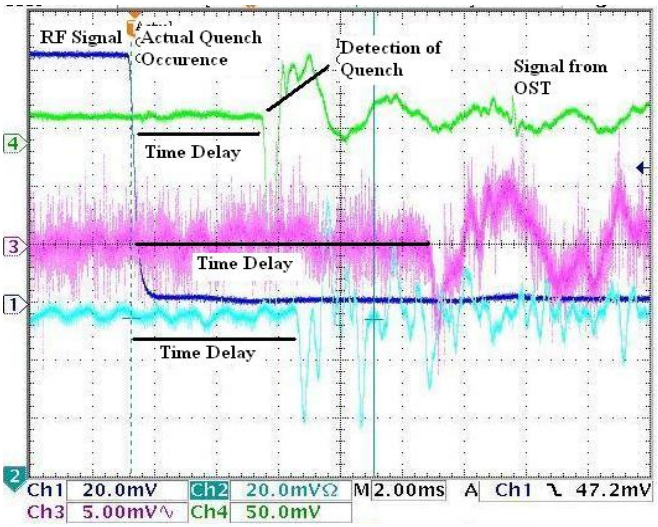

FIG. 9. A screen shot of the reading from oscilloscope which reads information from RF signal and three transducers. Channel 2 (cyan) corresponds to green AB, channel 3 (magenta) corresponds to orange AB and channel 4 (green) corresponds to orange GH. Channel 1 (blue) represents the RF signal.

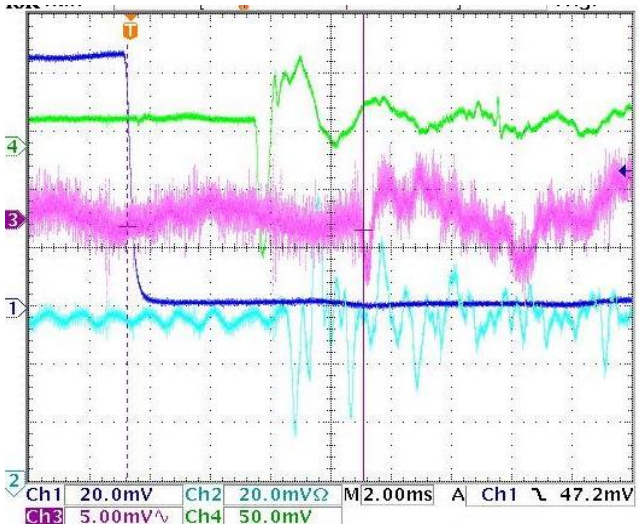

FIG. 10. A screen shot of the reading from oscilloscope which reads information from RF signal and three transducers. Channel 2 (cyan) corresponds to green AB, channel 3 (magenta) corresponds to green GH and channel 4 (green) corresponds to orange GH. Channel 1 (blue) represents the RF signal.

Figures (9) and (10) are the signal readings from a cold test of a single cell cavity. The quench occurred at the gradient of about 33.7 MV/m. We observed that

the time delay for second sound readings for green AB, green GH, orange AB and orange GH are 5.28 ms, 7.84 ms, 9.48 ms and 4.32 ms respectively. For this case, the reading was taken at the temperature 1.9K. The velocity of the second sound at this temperature of He II will be 17.5m/s. We can easily calculate the distance of the quench from the three transducers as 9.24 cm, 13.72 cm, 16.59cm and 7.56 cm respectively. Now, we can enter the locations of the three transducers in a coordinate system in which the center of the cavity is the origin and then find the quench location by the algorithm explained in the earlier section. Our calculation for this case shows that the quench should be located on the cavity at the point (1.229, 8.741, 7.324) in centimeters and is displayed on the cavity as in figure (12).

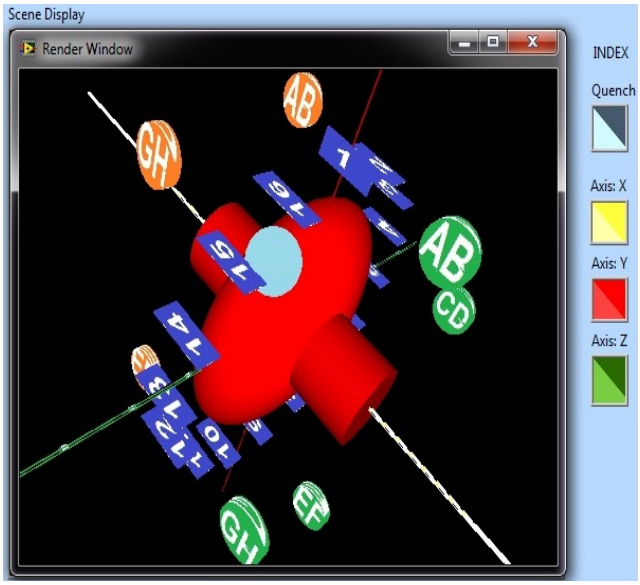

FIG. 11. Screen-shot of a computer 3D display of the quench on the cavity. Green and Orange transducers and RTDs (in blue) are shown for reference.

VII.2. Verification

It has been already explained that we have 16 Resistance Thermal Detectors (RTDs) along the equator of the cavity. For this experiment, the temperature gradient was observed on the RTDs 14, 15 and 16. Now, we can refer to the map of the cavity at figure (8) and locate the region in the cavity that should have the quench. We can affirm that the quench should be located on the area that is closer to the above stated RTDs . This is exactly the expected location based on the calculation using trilateration. Now, one can perform optical testing and then clean up the defect with electro-polishing or any other technique.

VIII. CONCLUSION

Hence, it was observed that we can use triangulation for a good approximation of the quench location of a single cell cavity. LabVIEW was also effective to perform the expected computation and displays. Also, the quantitative study of the effectiveness of the algorithm can be performed by optical tests and getting the actual location of the quench and compare it with the computed location. Another step from this project can be performing the 9-cell cavity test using OSTs. This will speed up the process of quench detection on the cavities. Nevertheless, there might be some complexities in such tests due to the cases like multiple quenching. But, it is encouraged that such tests shall be carried out and the studies should be done on them.

It also needs to pointed out that the algorithm I worked requires the second sound signal be read by four transducers. If we can devise some equation that provides the cavity geometry, then we might be able to lower the number to three transducers to locate the quench. For next phase, using MATLab might be a better option which allows a programmer to perform numerical analysis and approximations based on the geometry of the cavity and location of the quench and the transducers. This can help one to identify the quench location by using as few as two transducers with signal and the cavity geometry.

IX. ACKNOWLEDGMENT

I would like to express my sincere gratitude to my mentor, Elvin Harms whose advice, support and direction made this project possible. I would also like to thank Helen Edwards and other staffs of Fermilab-A0 facility whose were always ready to help in need and also made my early weeks of transition easy. Also, I would like to thank Eric Prebys and Linda Spentzouris for managing the internship and arranging various programs that were integral part of learning during the internship. I would like to thank Lee Teng for his contribution on making this internship possible. I would like to thank William Barletta and the USPAS team. I would also like to thank Carol Angarola for putting everything together and helping out with paperworks, housing, etc. I would also like to thank Erik Ramberg and Roger Dixon for their Wednesday meeting sessions which were full of exciting discussions on particle physics. Also, I would like to thank fellow interns for making the internship duration memorable

X. APPENDIX

1. Calculation of efficiency of transducer:

$$\begin{aligned}\frac{E_2}{E_1} &= \frac{\rho_n\nu_{n2}^2+\rho_s\nu_{s2}^2}{\rho\nu_{n1}^2} = \frac{\rho_n\nu_{n2}^2+\rho_s\nu_{s2}^2}{\rho_n\nu_{n1}^2+\rho_s\nu_{n1}^2}\,[\rho=\rho_n+\rho_s]\\ &= \frac{\rho_n\nu_{n2}^2+\rho_n\nu_{n2}^2}{\rho_n\nu_{n1}^2+\rho_s\nu_{n1}^2}\,\left[\rho_n\nu_{n2}=-\rho_s\nu_{s2}\rightarrow\rho_n\nu_{n2}^2=\rho_s\nu_{s2}^2\right]\\ &= \frac{2\rho_n\nu_{n2}^2}{\rho_s\nu_{s1}^2+\rho_s\nu_{n1}^2}\,[Similarly,\rho_n\nu_{n1}^2=\rho_s\nu_{s1}^2]\\ &= \frac{2\rho_n\nu_{n2}^2}{\rho_s\nu_{n1}^2+\rho_s\nu_{n1}^2}\left[E_1=\frac{\rho\nu_{n1}^2}{2}=\frac{\rho\nu_{s1}^2}{2}\rightarrow\nu_{n1}^2=\nu_{s1}^2\right]\\ &= \frac{\rho_n\nu_{n2}^2}{\rho_s\nu_{n1}^2}=\left(\frac{\rho_n}{\rho_s}\right)\left(\frac{\nu_{n2}}{\nu_{n1}}\right)^2\end{aligned} \tag{30}$$

2. From boundary condition- $\nu_{n1}=\nu-\nu_{n2}$

$$\begin{aligned}\rho\nu_{n1} &= \rho\nu-\rho\nu_{n2}=\nu(\rho_n+\rho_s)-\nu_{n2}(\rho_n+\rho_s)\,[\rho=\rho_n+\rho_s]\\ &= \nu\rho_n+\nu_{n1}\rho_s+\nu_{n2}\rho_s-\nu_{n2}\rho_n-\nu_{n2}\rho_s\,[\nu=\nu_{n1}+\nu_{n2}]\\ &= \nu\rho_n+\nu_{s1}\rho_s+\nu_{s2}\rho_s\,[\nu_{n1}=\nu_{s1},\nu_{n2}\rho_n=-\nu_{s2}\rho_s]\\ &= \nu\rho_n\,[\nu_{s1}+\nu_{s2}=0]\end{aligned} \tag{31}$$

and,

$$\rho\nu_{n2}=\nu\rho_s \tag{32}$$

Hence, from (26), (27) and (28):

$$\frac{E_2}{E_1}=\frac{\rho_n}{\rho_s}\left(\frac{\nu\rho_s}{\rho}\frac{\rho}{\nu\rho_n}\right)^2=\frac{\rho_s}{\rho_n} \tag{33}$$

[1] B.. Aune, R. Bandelmann, and D. et all Bloess. Superconducting TESLA Cavities. *Physical Review Special Topics-Accelerators and Beams*, 3:092001–1 – 092001–25, 2000.

[2] Z.A. Conway, l C.P. Hartil, H.S. Padamsee, and E.N. Smith. Defect Llocation in Ssuperconducting Cavities Cooled with He-ii using Oscillating Superleak Transducers.

[3] J.C. Han, B.J. Park, W.Y. Lee, H. Han, Y.J. Kim, S.B. Kim, C.S. Kim, and B.W. Lee. Photoacoustic Effect at Second-order Phase Transtition in $la_1-xca_xmno_3$. *Journal of Magnetism and Magnetic Materials*, 242-245:716–718, 2002.

[4] D.R. TIlley and J. Tilley. *Helium II: The Two-fluid Model*. Graduate Students Series in Physics. Institute of Phyiscs Publishing, 2003.

[5] New Effect Observed in Liquid Helium. *New Scientist*, 14:238, 1962.

[6] R.A. Sherlock and D.O. Edwards. Oscillating Superleak Second Sound Transducers.

[7] Sydney Yuan. Superfluid helium. `http://www.yutopian.com/Yuan/HeII.html`.

[8] Eric W. Weisstein. Gaussian Elemination. `http://mathworld.wolfram.com/GaussianElimination.html`.